



Study of Different Heating Effects on Two-Phase Flow of Magnetized Couple Stresses Over a Permeable Stretching Cylinder with Velocity Slip and Radiation

Mahesh Garvandha¹ · G. Nagaraju² · Devendra kumar¹ · Ali J. Chamkha³

Accepted: 22 July 2022

© The Author(s), under exclusive licence to Springer Nature India Private Limited 2022

Abstract

The couple stresses of a dusty fluid across a stretching cylinder are investigated using a mathematical model. The governing flow is 2-dimensional in nature and the cylinder is submerged in a porous medium. Effect of radiation, slip velocity, viscous energy dissipation, Newtonian, and Joule heating are incorporated in our mathematical model. The flow system is governed by basic partial differential equations. Our model's governing equations are translated to coupled nonlinear ordinary differential equations using similarity transformations, which are then solved using the Runge–Kutta Fehlberg iterative technique. Variations in velocity and thermal gradient under the influence of relevant parameters are examined numerically and are illustrated graphically. The non-dimensional skin shear stress (coefficient of skin friction) and the rate of heat transfer are calculated for permeable flow over the cylinder for different flow parameters and are displayed through a table. Later, the numerical results obtained are compared to the results available in literature and found to be in reasonable accord. Results indicate that, the rising of coupling parameter values upsurges the fluid velocity but declines the temperature of both phases (fluid and dust). Enhanced thermal profiles are observed with Newtonian heating parameter in two fluid mixtures. The temperature enhances with increasing the radiation parameter where it decreases for increasing the magnetic field parameter and specific heat ratio. Additionally, the rate of heat transfer reduces for higher values of mass concentration and velocity interaction parameter.

Keywords Couple stresses · Two-fluid model · Stretchable cylinder · Porous medium · Slip velocity · Newtonian heating

Abbreviations

B_0 Constant magnetic field

✉ G. Nagaraju
naganitw@gmail.com

¹ University of Technology and Applied Sciences-Shinas, Shinas, Sultanate of Oman

² Department of BSH, Vaagdevi College of Engineering, Bollikunta, Warangal, Telangana, India

³ Faculty of Engineering, Kuwait College of Science and Technology, 35004 Doha, Kuwait

B	Slip parameter
Ec	Eckert number
K	Stoke's resistance constant ($6\pi r\mu$)
K_p	Permeability parameter
k	Thermal conductivity ($Wm^{-1} K^{-1}$)
k'	Permeability of the medium (m^2)
l	Characteristic length
l^*	Parameter of mass concentration
M	Magnetic number
m	Mass of dust particles
N	Density number(dust particle)
Pr	Prandtl number
Re	Reynolds number
Rd	Radiation parameter
s	Couple stresses parameter
T, T_p	Fluid and dust particle temperature
T_0	Reference temperature
T_∞	Ambient temperature
U_0	Reference velocity
$(u, w), (u_p, w_p)$	Components of velocity in (r, z) directions

Greek symbols

β	Interaction parameter(velocity)
β_T	Interaction parameter for temperature
γ	Curvature parameter
γ_1	Specific heat parameter
λ	Conjugate parameter of Newtonian heating
μ	Dynamic viscosity
ρ, ρ_p	Fluid and particle phase density(with $\rho_p = mN$)
τ_T	Thermal equilibrium time
τ_v	Time relaxation of particle phase

Introduction

The study of two-phase flow has been quite important due to the huge number of applications in chemical engineering systems that enables improvement in design and ensures their safe operation. The listed applications of two-phase dusty fluid flow (suspensions of dust particles in clean fluid) are two-phase propulsions, sedimentation, and cement, and steel manufacturing industries, dynamics of the atmosphere, film cooling systems, environmental pollution, fluidized beds, genetic mutation, and blood rheology. Saffman [1] initially developed the equation of motion and explored dusty fluid stability. Chakrabarti [2], Vajravelu and Nayfeh [3], Chamkha [4], Attia [5], Damseh [6], Ezzat et al. [7] carried out numerical and analytical examinations of dusty fluid flow processes. Gireesha et al. [8–10] examined stretching effect of linear and exponential in nature for porous as well as non-porous sheets in dusty fluid transport phenomenon. The authors conducted the investigations for thermal radiation, heat

generator/absorber parameter, viscous dissipation etc. Manjunatha et al. [11] investigated MHD dusty flow through cylinders of stretched surfaces with thermal and radiation effects. The authors observed reverse effects of increasing permeability parameter for both the phases. Turkyilmazoglu [12] found the exact solution for deforming isothermal surfaces. The slip and radiation effects of dusty hybrid nanoparticle flow over stretching surface are numerically studied by Souayah et al. [13]. They discovered that at higher values of the slip parameter, the velocity profile for both the fluid and dusty phases is reduced. Rashed [14] used two circular cylinders with varying heat conditions to examine how to impact three-dimensional dusty flow of nanofluid. He noticed that as the Hartmann number rises, the temperature gradients become more significant. Muhammad Ibrahim et al. [15] investigated the two-phase analysis of heat transmission and entropy generation in a twisted porous block-filled circular micro-tube. A closed-form solution for Jeffery multiphase flow in a sloping channel was obtained by Nazeer et al. [16]. They discovered that Jeffrey-based multiphase flow has better velocity profile than Newtonian-based multiphase flow.

Non-Newtonian fluids are currently garnering a considerable interest among scientists. Physical applications in several engineering fields have inspired this interest. Non-Newtonian fluids are used in production of paper, fiber technology, electromagnetic material processing, cosmetic operations, hot rolling, oil reservoirs, medications, and other applications. Various models have been developed to understand the behavior of non-Newtonian fluids. Among these, the couple stress theory projected by Stoke's includes the incidence of couple stress, asymmetric stress tensor, body forces, and body couples. The assumption of a size-dependent consequence that does not fit within the non-polar theory, distinguishing couple stresses. This type of fluids can be used to study the mechanism of lubrication of synovial joints (Walicki and Walicka [17]) along with exploration of different kinds of lubricants, blood suspension fluids, etc. In the procedure, the couple stress fluid is used to solidify liquid crystals, colloidal solutions, cooling metallic plate, and extruding polymer fluids. The couple stress model can also be applied to biomechanical problems. Those certain impressive papers in couple stresses by various geometries can even be found in the work of Nagaraju and Ramana murthy [18], Nagaraju et al. [19], Asad et al. [20], Jangili et al. [21]. Agarwal and Anushri [22] studied on couple stress fluid for thermal instability caused Hall current and mixture of dust particle. It is found that system is stabilized by couple stress. Stanly and Vasantha [23] investigated the application of external heat source provided to couple stresses second order fluid through porous medium under the solute gradient. The authors put light on stability of rotating couple stress of second order fluid with applied magnetic field. Thermal convections also stabilizing by magnetic field applications. Nagaraju and Nandkeolyar [24] analyzed the effects of MHD, viscous heating and suction of time dependent dusty couple stress fluid over a stretching flat sheet. They discovered that as the magnetic field parameter values increased, the thickness of the momentum boundary layer shrank. Very recently, Uma et al. [25] examined the impacts of couple stress, Thermophoresis parameter, radiation absorption parameter, heat absorption parameter on Couette flow in a wavy plate for two-phase fluid. They identified that with rise of radiation absorption, the temperature and velocity profiles enhance. Dogonchi and his co-researchers [26–30] have provided an explanation of the impacts of nanoparticle migration on annulus between the cylinder and rhombus/circular wavy wall caused by temperature gradient on the motion of nano fluid.

Study of the fluid transport through stretching plates and stretching cylinders are important due to their applications in fiber technology, glass blowing, metal spinning, paper production, revolving tube heat exchangers, polymer discharge, and drawing plastic films. The boundary layer inflow sophistications and heat transfer rates at the surfaces which are stretched are veritably important application for the quality of the final product. Sakiadis[31] first derived

the boundary layer basic equations for the moving solid surfaces. Later Crane [32] extended Sakiadis's concept and found a valid solution at large axial distances. Wang [33] studied axisymmetric exterior fluid flow of stretching hollow cylinder. Following then, numerous researchers looked at various aspects of the problem and came up with identical solutions. For a long time, heat transfer flows in a porous material have been an attractive study area, as seen by the large number of articles published. Mukhopadhyay [34] has shown the results for influence of permeability parameter on flow field. Chauhan et al. [35] researched magneto hydrodynamic slip inflow and heat transmission over a permeable material across a stretching surface. Researchers have also explored various aspects of heat transport through a stretching cylinder with various types of fluid models. Nandkeolyar and Sibanda [36] considered the viscous and Joule dissipations and showed that dusty fluid flow is influenced by these parameters in the stretching surface. The differential transform method was used by Deepa Sinha et al. [37] to analyze the analytical two-dimensional solution for the nanofluid heat transfer model. The effects of viscous heating and Darcy-Forchheimer on hybrid nanofluid flow with suspended dust particles were investigated by Punith Gowda et al. [38]. They observed that the porosity parameter increases heat transmission in both phases while decreasing the velocity gradient for both phases. Gangadhar et al. [39] studied the Ferro magnetic heat transfer flow with radiation and convective boundary condition. Authors concluded that radiation increases with the rise in Hartmann number. Masood Khan et al. [40] investigated MHD flow over an inclined stretched cylinder with slip effects. They discovered that as the slip parameter rises, the skin shear stress decelerates. The impacts of thermal radiation and non-uniform heat flux on MHD hybrid nanoparticle over a stretching surface were explored by Aamir Ali et al. [41]. They found that as the radiation parameter upsurges, the temperature of the fluid enhances. Different approaches are used to address the phenomenon of highly coupled nonlinear differential equations developed in various stretchable nanofluid models are found in Ellahi et al. [42–45].

Different studies have extensively used Newtonian heating phenomena to design and create heat exchangers, conjugate convective heat transfer around fins, and convection overflows during which boundary shells absorb radiation from another object. Those certain impressive papers in boundary layer flow with Newtonian heating and dissipation can even be found in Makinde [46], Farooq et al. [47], Hayat et al. [48], Hayat et al. [49]. When an electric current passes through a conducting substance and produces heat, this is known as Joule heating. This is due to the interaction (i.e., collision) between the moving particles. Consequently, some of the energy is transferred to heat, which raises the body's temperature. In recent years, scientists and researchers have been focused on improving the efficiency of a variety of mechanical systems and industrial equipment. Such problems can be overcome by reducing the temperature generated by Joule heating, and heat source/sink. Awaz et al. [50] studied the effect of Joule and Newtonian heating on stretching surface. Recently Misra et al. [51] examined the effect of Joule dissipation on MHD Casson fluid. They discovered that as Casson fluidity increases, the temperature of the fluid falls. Ree-Eyring fluid flow between two stretchable rotating discs was obtained by Zhao et al. [52] for the nonlinear mixed convective entropy-optimized electrical conducting flow.

Numerous industrial and mechanical applications such as fire engineering, nuclear reactors, and combustion modeling use heat transport in radiated electrical conducting flows, which are most significant classes of boundary layer theory problems. Engineers and scholars have been examining the crucial aspects of fluid flow and heat transfer under a variety of assumptions for the past number of decades. In view of the above applications; one can feel that attention has been paid to the multiphase flow of couple stress fluid. Further, no bi-phase flow has been reported so far which is composed of couple stress fluid as the base liquid.

In addition to this, no comparative analysis between non-Newtonian multiphase flows is present in the existing literature. Motivated by the above facts, a successful attempt has been made to analyze magneto hydrodynamics of multiphase non-Newtonian fluid flow through a stretched cylinder. The literature review conveys that hydro magnetic influence on the permeable stretched flow of dust particles over a cylinder subject to couple stresses, radiation, velocity slip, Joule and Newtonian heating is yet to be explored. The goal of the current communication is to examine and make readers aware of how various factors, including the magnetic parameter, the permeability number, radiation parameter, the Newtonian heating parameter, the couple stresses parameter, the specific heat ratio parameter, the slip parameter, the mass concentration parameter, the velocity interaction parameter, and the type of flow, affect thermal transport in the dusty flow towards a cylinder's surface. It is hoped that this would lead to a greater comprehension of the existing understanding of heat transport and enable scientists and engineers to develop the kinds of mathematical modeling needed to achieve the desired heat transport-related goals. The Runge–Kutta Fehlberg iterative approach [53–55] is used to solve numerically the desired ordinary differential equations.

Mathematical Model

Consider a 2-dimensional, time independent, incompressible flow of couple stress dusty fluid over a stretching cylinder in porous medium. The cylindrical coordinate system is adopted in such a way that z -axis is considered as flow direction and r -axis towards the radial direction as in Fig. 1.

A strong constant magnetic field is applied along the radial direction which is normal to the flow field. Newtonian heating and velocity slip is entailed at the stretching cylinder. The effect of Joule heating, radiation, and viscous dissipation are assumed in the energy equation. The governing equations stated below under the assumptions, and boundary layer approximations [Turkyilmazoglu [12], Nagaraju et al. [24], Makinde [46] and Farooq et al.

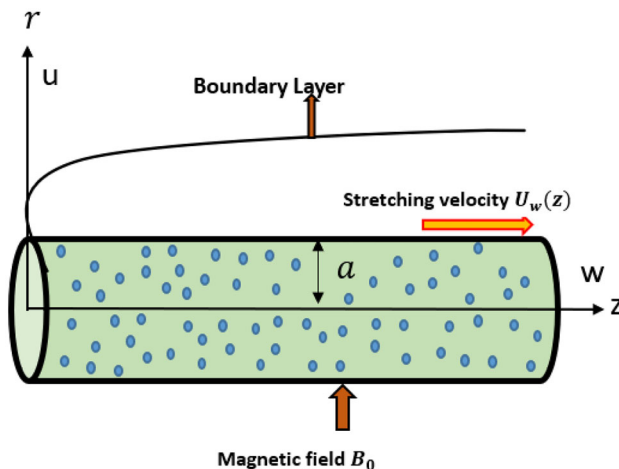


Fig. 1 Schematic diagram of flow of couple stress dusty fluid

[47]] are:

$$\frac{\partial u}{\partial r} + \frac{u}{r} + \frac{\partial w}{\partial z} = 0 \tag{1}$$

$$u \frac{\partial w}{\partial r} + w \frac{\partial w}{\partial z} = \frac{\mu}{\rho} \left(\frac{\partial^2 w}{\partial r^2} + \frac{1}{r} \frac{\partial w}{\partial r} \right) - \frac{\eta_0}{\rho} \left(\frac{\partial^4 w}{\partial r^4} + \frac{2}{r} \frac{\partial^3 w}{\partial r^3} - \frac{1}{r^2} \frac{\partial^2 w}{\partial r^2} + \frac{1}{r^3} \frac{\partial w}{\partial r} \right) + \frac{KN}{\rho} (w_p - w) - \frac{\sigma B_0^2 w}{\rho} - \frac{\mu}{\rho k'} w \tag{2}$$

$$u_p \frac{\partial w_p}{\partial r} + w_p \frac{\partial w_p}{\partial z} = \frac{K}{m} (w - w_p) \tag{3}$$

$$\frac{\partial(u_p)}{\partial r} + \frac{u_p}{r} + \frac{\partial(w_p)}{\partial z} = 0 \tag{4}$$

$$\rho C_p \left(u \frac{\partial T}{\partial r} + w \frac{\partial T}{\partial z} \right) = k \left(\frac{\partial^2 T}{\partial r^2} + \frac{1}{r} \frac{\partial T}{\partial r} \right) + \frac{\rho_p C_m}{\tau_T} (T_p - T) + \mu \left(\frac{\partial w}{\partial r} \right)^2 + \frac{\rho_p}{\tau_v} (w_p - w)^2 - \frac{1}{r} \frac{\partial}{\partial r} (r q_r) + \sigma B_0^2 w^2 \tag{5}$$

$$\rho_p C_m \left(u_p \frac{\partial T_p}{\partial r} + w_p \frac{\partial T_p}{\partial z} \right) = -\frac{\rho_p C_m}{\tau_T} (T_p - T) \tag{6}$$

The boundary constraints are defined as

$$w = U_w(z) + B_1 v \frac{\partial w}{\partial r}, u = 0, \frac{\partial T}{\partial r} = -h_s T \text{ at } r = a \tag{7}$$

$$w \rightarrow 0, w_p \rightarrow 0, u_p \rightarrow u, \frac{\partial w}{\partial r} \rightarrow 0, \frac{\partial^2 w}{\partial r^2} \rightarrow 0, T \rightarrow T_\infty, T_p \rightarrow T_\infty \text{ as } r \rightarrow \infty \tag{8}$$

where $U_w(z) = \frac{U_0 z}{l}$ = stretching cylinder velocity, $T = T_w = T_\infty + \frac{T_0 z}{l}$ = surface temperature. The Stokesian drag force is employed for the contact between the fluid and particle phases, and the induced magnetic field is omitted in the equations. Similarly, the external electric field is zero, and the electric field generated by the polarization charge is negligible.

The following appropriate variables are suggested as

$$w = \frac{U_0 z}{l} f', u = \frac{-a}{r} \left(\frac{U_0 v}{l} \right)^{\frac{1}{2}} f(\eta), \eta = \frac{r^2 - a^2}{2a} \left(\frac{U_0}{vl} \right)^{\frac{1}{2}}, \theta(\eta) = \frac{T - T_\infty}{T_\infty}, \theta_p(\eta) = \frac{T_p - T_\infty}{T_\infty}, w_p = \frac{U_0 z}{l} F', u_p = -\frac{a}{r} \left(\frac{U_0 v}{l} \right)^{\frac{1}{2}} F(\eta). \tag{9}$$

Using Eq. (9) in the Eqs. (2–6), we are having:

$$(1 + 2\eta\gamma) f''' + 2\gamma f'' + f f'' - (f')^2$$

$$-s Re \left((1 + 2\eta\gamma)^2 f^v + 8\gamma(1 + 2\eta\gamma) f^{iv} + 8\gamma^2 f''' \right) + l^* \beta (F' - f') - (M^2 + K_p) f' = 0 \tag{10}$$

$$-(F')^2 + F F'' + \beta (f' - F') = 0 \tag{11}$$

$$\frac{(1 + Rd)}{Pr} \left[(1 + 2\eta\gamma)\theta'' + 2\gamma\theta' \right] + f\theta' - f'\theta + l^*\gamma_1\beta_T(\theta_p - \theta) + Ec \left\{ (1 + 2\eta\gamma)(f'')^2 + l^*\beta(F' - f')^2 + M^2(f')^2 \right\} = 0 \tag{12}$$

$$-F\theta'_p + F'\theta_p + \beta_T(\theta_p - \theta) = 0. \tag{13}$$

The below listed boundary conditions obtained from Eqs. (7–8)

$$f = 0, f' = 1 + Bf'', \theta' = -\lambda(1 + \theta) \text{ at } \eta = 0 \tag{14}$$

$$f' = F'' = F - f = f'' = f''' = \theta = \theta_p = 0 \text{ as } \eta \rightarrow \infty \tag{15}$$

where $= \frac{\eta_0}{\mu a^2}, \gamma = \left(\frac{\nu l}{a^2 U_0} \right)^{\frac{1}{2}}, M^2 = \frac{\sigma l B_0^2}{\rho U_0}, Re = \frac{U_0 a^2}{\nu l}, l^* = \frac{\rho_p}{\rho}$ with $\rho_p = mN, \beta = \frac{l}{\tau_w U_0}$

with $\tau_w = \frac{m}{K}, K_p = \frac{l\nu}{U_0 k^*}, B = B_1 \left(\frac{U_0 \nu}{l} \right)^{\frac{1}{2}}, \lambda = h_s \left(\frac{U_0}{\nu l} \right)^{-\frac{1}{2}}, Pr = \frac{\mu c_p}{k}, \beta_T = \frac{l}{U_0 \tau_T}, Ec = \frac{U_w^2}{c_p(T_w - T_\infty)},$

$$Rd = \frac{16\sigma^* T_\infty^3}{3kk^*}, \gamma_1 = \frac{C_m}{C_p}.$$

The simplified terms for dimensionless Skin shear stress and Nusselt number are given by.

$$C_f = \frac{2\tau_w}{\rho U_w^2}, Nu = \frac{zq_w}{k(T_w - T_\infty)}, \text{ where.}$$

$$\tau_w = \mu \left(\frac{\partial w}{\partial r} \right)_{r=a} \text{ and } q_w = \left(-k \frac{\partial T}{\partial r} \right)_{r=a} + (q_r)_{r=a}.$$

In non-dimensional form,

$$\frac{1}{2} C_f \sqrt{Re_z} = f''(0) \tag{16}$$

$$\frac{Nu_z}{\sqrt{Re_z}} = -(1 + Rd)\theta'(0) \tag{17}$$

where $Re_z = \frac{U_w z}{\nu}$.

Solution Procedure

The non-linear coupled expressions (10–13) are converted to system of first order initial value problem before implementing Runge–Kutta Fehlberg method. The below procedure was employed to obtain first order initial value problem.

$$f = y_1, f' = y_2, f'' = y_3, f''' = y_4, f'''' = y_5, F = y_6, F' = y_7, \theta = y_8, \theta' = y_9, \theta_p = y_{10} \tag{18}$$

$$f^v = \left(\begin{matrix} (1 + 2\eta\gamma)y_4 + 2\gamma y_3 + y_1 y_3 - y_2^2 - 8sRe\gamma(1 + 2\eta\gamma)y_5 \\ -8sRe\gamma^2 y_4 + l^*\beta(y_7 - y_2) - (M^2 + K_p)y_2 \end{matrix} \right) / (sRe(1 + 2\eta\gamma)^2), \tag{19}$$

$$F'' = (y_7^2 - \beta(y_2 - y_7))/y_6, \tag{20}$$

$$\theta'' = -(y_1 y_9 - y_2 y_8 + l^*\gamma_1\beta_T(y_{10} - y_8) + Ec \{ (1 + 2\eta\gamma)y_3^2 + l^*\beta(y_7 - y_2)^2 + M^2 y_2^2 \} + 2(1 + Rd)\gamma y_9 / Pr) / ((1 + Rd)(1 + 2\eta\gamma) / Pr), \tag{21}$$

$$\theta'_p = (\gamma_7 y_{10} + \beta_T (y_{10} - y_8)) / y_6. \tag{22}$$

With the proper boundary conditions in place,

$$y_1 = 0, y_2 = 1 + B y_3, y_9 = -\lambda(1 + y_8) \text{ at } \eta = 0, \tag{23}$$

$$y_2 = y_7 = y_6 - y_1 = y_3 = y_4 = y_8 = y_{10} = 0 \text{ as } \eta \rightarrow \infty. \tag{24}$$

Most of the boundary conditions are specified at the right end, authors start the integration at $\eta \rightarrow \infty$ i.e. sufficiently large value is $\eta = 6$ and proceed with negative step size towards $\eta = 0$. Authors guessed the values of y_1, y_5, y_9 at right end by shooting technique, after that obtained the solutions of Eqs. (18–22) using Runge–Kutta Fehlberg technique with step size–0.01. The accuracy was obtained for our method.

Results and Discussion

The impact of various pertinent parameters for axial velocity and thermal profiles in fluid and dust phases are shown graphically and the results have theoretically deliberated. All the graphs are plotted using solid lines for fluid phase where dotted lines representing dust phase. The effect of curvature parameter (γ) is illustrated in Fig. 2 and it shows that velocity profiles, temperature field of fluid and dust phase flow increase as γ increases. Both the velocity profiles and temperature fields are declined heavily for η from 0 to 2 while very low for $\eta \geq 2$. In fact, as γ raise, the radius of the curvature decreases, that reduces the contact surface between cylinder and the fluid, resulting in lower fluid flow resistance.

Figure 3 describes the influence of Re on velocity and temperature profiles in both phases. One can see that an escalating value of Re enhances the velocity profile and decelerates the thermal energy of both phases. This is because of inertial forces and the fluid velocity that is directly proportional to the Reynolds number.

From Fig. 4, it is noticed that the velocity profile enhances and, the thermal profile declines for rising values of couple stress parameter(s). This is because the couple stress along with curvature and slip gives bending deformation which enhances the velocity and due to reduced contact surface area temperature reduced.

Figure 5 illustrates that the velocity profile enhances and the temperature profile declines

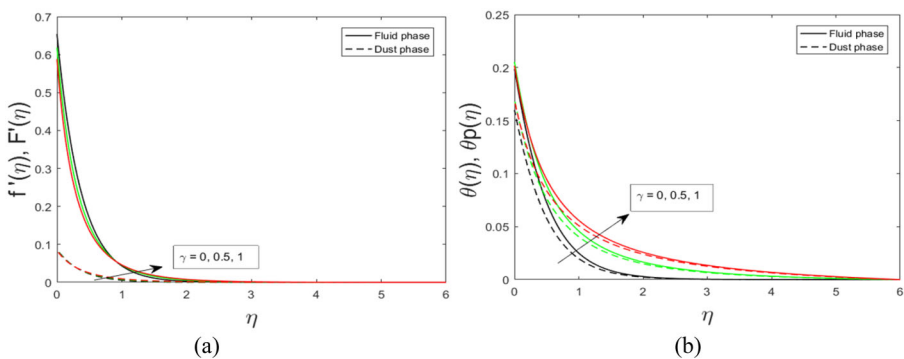


Fig. 2 Effect of γ on **a** axial velocity **b** Temperature profile

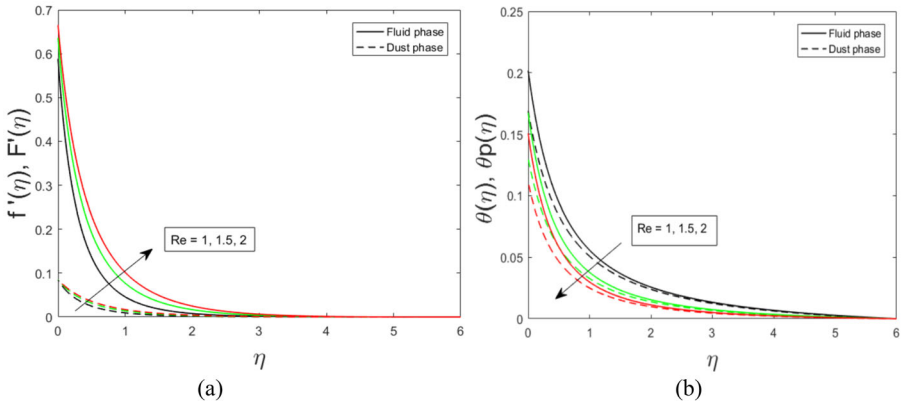


Fig. 3 Effect of Re on **a** axial velocity **b** Temperature profile

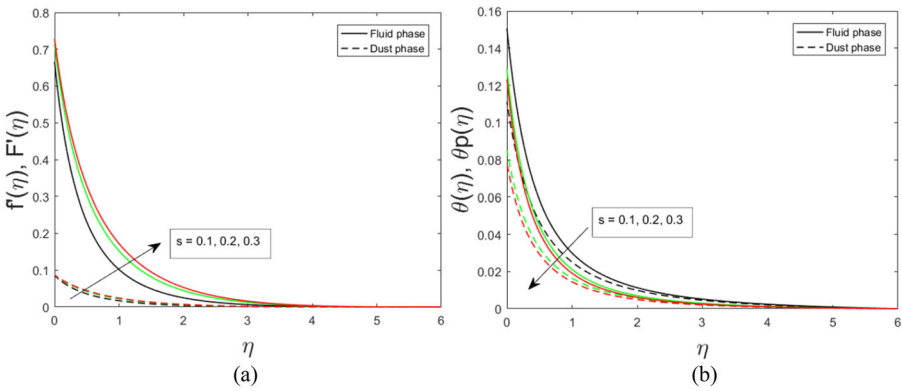


Fig. 4 Effect of s on **a** axial velocity **b** Temperature profile

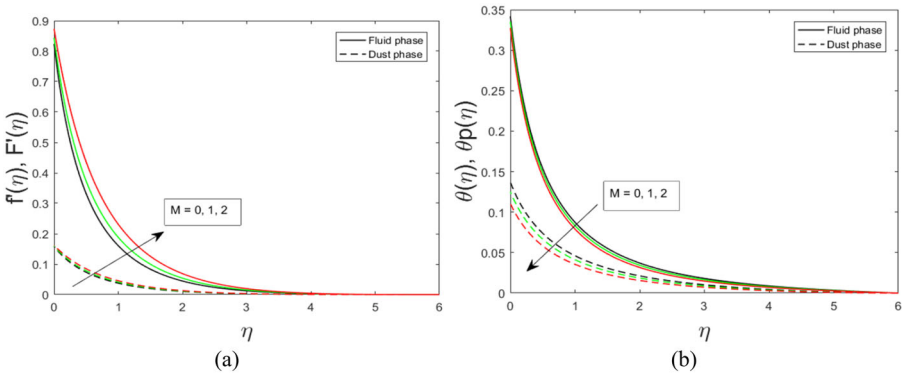


Fig. 5 Effect of M on **a** axial velocity **b** Temperature profile

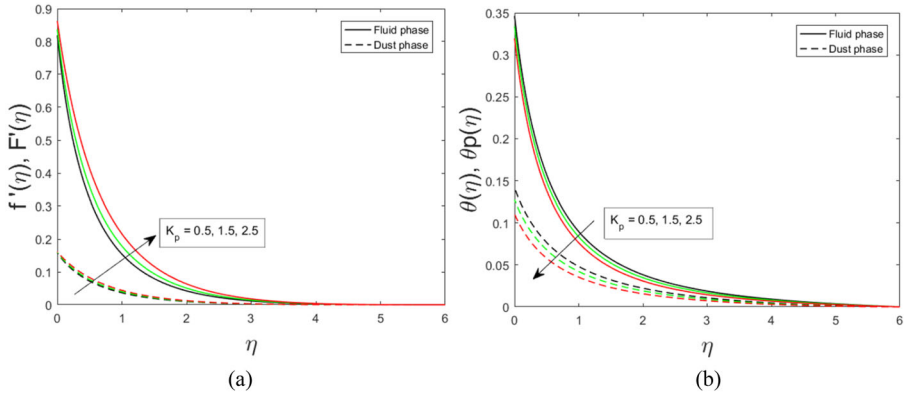


Fig. 6 Effect of K_p on **a** axial velocity **b** Temperature profile

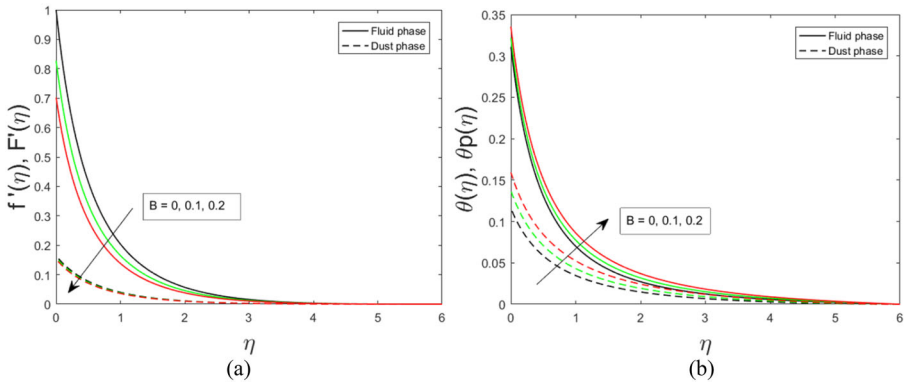


Fig. 7 Effect of B on **a** axial velocity **b** Temperature profile

for increasing values of Magnetic parameter (M). In couple stress dusty fluid some disturbances are found due to stratifications. The magnetic field gives streamline flow to both phases.

The impact of the permeability parameter on velocity and thermal gradient in both the phases is sketched in Fig. 6. An increment in K_p enhances the velocity profile and reduces the temperature profile in both phases. This quality is dominant up to a certain point, after which the process slows down. It should be noticed that K_p has a significant impact on the solutions (flow streams). It is self-evident that the presence of permeability creates greater fluid restriction, lowering fluid velocity.

Figure 7 exhibit that the velocity profile declines, and the thermal gradient profile enhances as the velocity slip parameter (B) increases. The particle (suspensions) gains the velocity by carrying fluid so average difference decreases which declines the velocity of both the phases while temperature increases due to more interactions. The impact of β, l^* on velocity and thermal gradients in both the phases are plotted in Figs. 8, 9. The velocity profile enhances and temperature declines in both phases with the rise of β, l^* .

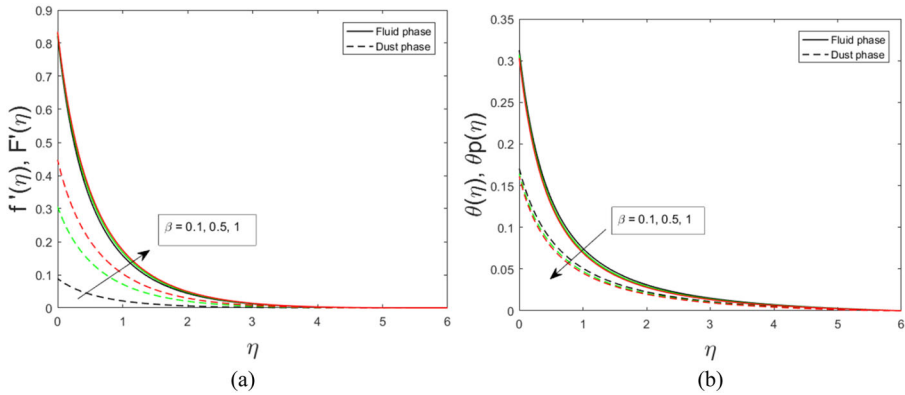


Fig. 8 Effect of β on a axial velocity b Temperature profile

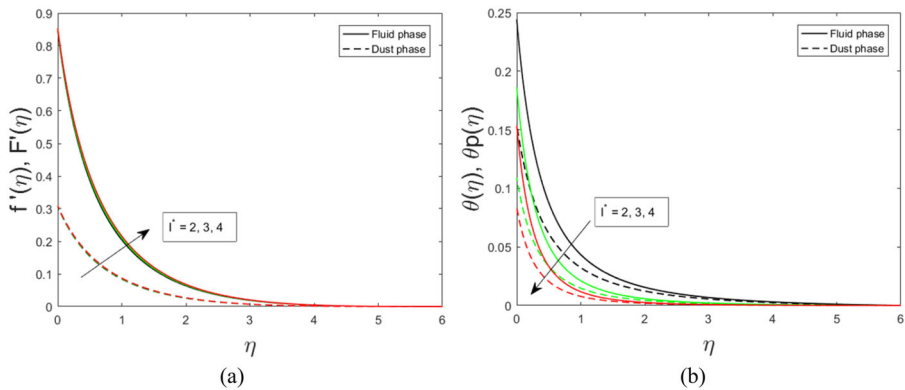


Fig. 9 Effect of l^* on a axial velocity b Temperature profile

The effect of the radiation parameter (Rd) on the temperature gradient of both the fluid and dust phases is depicted in Fig. 10a. The relative contribution of conduction heat transfer to thermal radiation transport is defined by the radiation parameter Rd . It is clear that an increase in the radiation parameter causes the temperature and velocity within the boundary layer to increase. As expected, the increase in the thermal radiation parameter enhances the thermal boundary layer thickness. Figure 10b exhibits the effect of Pr on the temperature field, here the temperature profile declines with the rising values of Pr . The Prandtl number evaluates the relationship between a fluid's capability for heat and momentum transport. The reduction in temperature distribution is caused by the fact that a larger Prandtl number Pr corresponds to a lower thermal diffusivity. As seen in Fig. 10c, an increase in the Eckert number Ec causes the thermal profile to rise. The Eckert number is used to describe heat dissipation in high-speed flows with strong viscous dissipation. Indeed, as Ec increases, the particles become more active as a result of energy conservation, which helps to raise the temperature profile. The influence of the conjugate parameter on thermal profiles is seen in Fig. 10d. It has been revealed that increasing the conjugate parameter causes energy profiles to rise. A higher λ increases the fluid's temperature to increase. The higher heat transfer

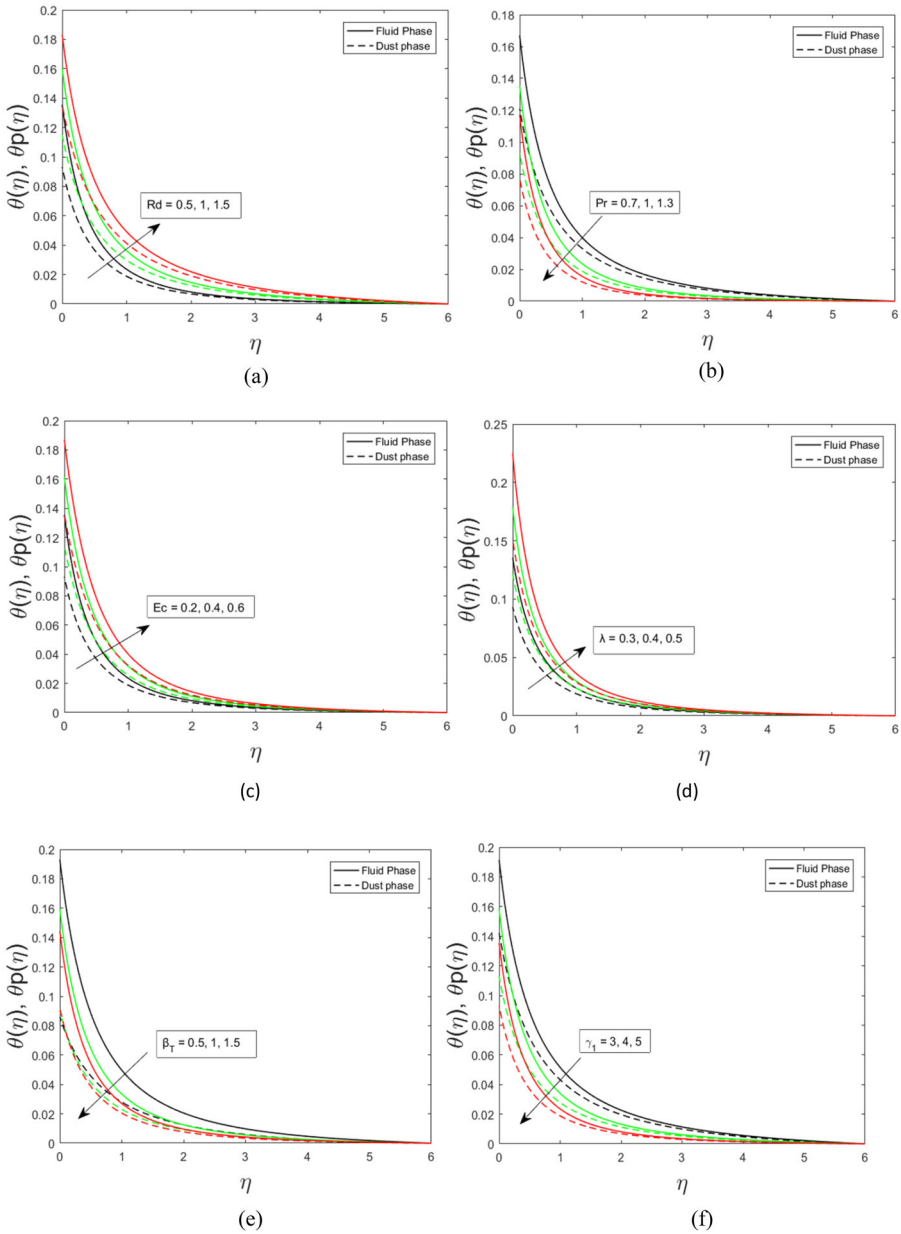


Fig. 10 Temperature profile variation for **a** Radiation parameter(Rd) **b** Prandtl number(Pr) **c** Eckert number(Ec) **d** conjugate parameter of Newtonian heating (λ) **e** Fluid interaction parameter for temperature(β_T) **f** Specific heat ratio(γ_1)

Table 1 Comparison of $-f''(0)$ for various values of M at $\gamma = 0, s = 0, B = 0, K_p = 0$

M	$-f''(0)$ Mukhopadhyay [34]	$-f''(0)$ Present values(Fehlberg method)
0	1.0000	1.0000
0.5	1.1180	1.1179
1	1.4142	1.4142
1.5	1.8027	1.8028

coefficient is the cause of this intensification. As a result, the fluid temperature rises. The fluctuations of $\theta(\eta)$ and $\theta_p(\eta)$ with β_T are shown in Fig. 10e. Rising values of β_T are seen to decrease the velocity and temperature profiles of both the fluid and dust phases. From Fig. 10f, it is evident that the thermal profile decelerates in both the phases for rising values of γ_1 .

Comparison of employed numerical scheme results of $-f''(0)$ for $B = 0$ (no slip), $s = 0, K_p = 0$, and $\gamma = 0$ with the outcomes of Mukhopadhyay [34] are listed in Table 1 and the present findings agree well. Table 2 demonstrates that the amplitude of skin shear stress increases as the γ increases, whereas larger values of M, s, Re , and K_p exhibit the opposite tendency. With an increase in Pr and γ , the heat transfer rate is depleted, whereas Rd increases the heat transfer rate.

Conclusions

This study explores the numerical investigation of two-phase dusty couple stress fluid flow over a stretching cylinder encapsulated in a permeable material in the presence of radiation, applied magnetic field, viscous dissipation, and Joule heating. Further, it also considers slip velocity and Newtonian heating at the boundary. To solve the converted non-dimensional equations, the Runge–Kutta Fehlberg iterative approach is used. In the RKF45 the solution converged in less number of approximations with significant truncation error. The significant outcomes are noted as:

- i. In the present study thermal radiation, slip condition, Newtonian and Joule heating effects are listed along with further external restrictions. Newtonian heating (λ) and thermal radiations (Rd) is enhancing the thermal transport and impacting the contact surface area, which are depicting motivational investigations.
- ii. In this investigation Newtonian heating (λ) and stretches of the contact surfaces (γ) have shown enhancing trend in temperature field while couple stress (s) declines the same.
- iii. Here flow and thermal transport are enumerated for slip condition. At the contact surface due to stretch and more interactions the temperature field is increasing and the velocity profile for both the phases is decreasing for increasing slip (B).
- iv. In the presence of Newtonian heating (λ) an enhancement is occurred in velocity profile for both the phases for rising values of $\gamma, Re, s, M, K_p, I^*, \beta$ and reverse trend appeared for increasing values of slip parameter.
- v. Rapid retardation appeared in the temperature profile for rising of $Re, M, K_p, \beta_T, Pr, \gamma_1$ and enhancing for escalating the values of γ, Ec .
- vi. When radiation is increasing, the velocity of both the phases increases where increasing Prandtl number (Pr) shows decreasing trends.

Table 2 Numerical values of $-f''(0)$, $-\theta'(0)$

γ	M	K_p	s	Re	Rd	Pr	β	l^*	βT	γ_1	B	λ	Ec	$-f''(0)$	$-\theta'(0)$
0	0.2	1	0.1	1	0.5	1	0.1	3	0.5	5	0.2	0.3	0.1	1.7283	0.3764
0.5														1.9079	0.3730
1														2.0586	0.3674
1	0	1	0.3	1	0.5	1	0.1	3	0.5	4	0.2	0.3	0.1	1.7622	0.6709
	1													1.5650	0.6675
	2													1.2647	0.6638
1	0.2	0.5	0.3	1	0.5	1	0.2	3	0.5	4	0.1	0.5	0.1	1.8095	0.6732
	1.5													1.6319	0.6671
	2.5													1.3709	0.6598
1	0.2	1	0.1	2	0.5	1	0.1	3	2	5	0.2	0.3	0.2	1.6721	0.3452
	0.2													1.4311	0.3387
	0.3													1.3565	0.3370
1	0.2	1	0.1	1	0.5	1	0.1	3	2	5	0.2	0.3	0.2	2.0586	0.3605
	1.5													1.8194	0.3502
	2													1.6721	0.3452
1	0.2	1	0.3	1	0.5	0.7	0.1	3	2	5	0.2	0.3	0.2	1.5112	0.3501
						1								1.5112	0.3406
						1.3								1.5112	0.3352
1	0.2	1	0.3	1	0.5	1	0.1	3	2	5	0.2	0.3	0.2	1.5112	0.3406
					11									1.5112	0.3481
					1.5									1.5112	0.3550
1	0.2	1	0.3	1	0.5	1	0.2	3	0.6	4	0	0.5	0.1	2.0461	0.6554
											0.1			1.7280	0.6608
											0.2			1.4886	0.6677

- vii. The fluid velocity is the source velocity for dust particles(suspensions), thus dust phase velocity is observed to be less than fluid phase velocity in all measurements.
- viii. Temperature profile enhances in both the phases for increasing values of Eckert number (Ec), fluid particle interaction parameter (β_T) and declines for higher specific heat(γ_1).
- ix. In this current investigation of Newtonian heating surface resistance as well as internal resistance between two phases is found to be decreased and transport of fluid is enhanced.

Above results are mostly belong to petroleum industry, oil extraction from oil wells as well as fiber industry. These results may be practically incorporated by the industry under the consultation of experts. The future scope of this work can be a comparative study of experimental outcomes within numerical limits.

Funding The authors declare that funding information is not available for this article.

Data availability The authors declare that the data supporting the findings of this study are available within the article.

Declarations

Conflict of interest The authors declare that we have no competing interests.

References

1. Saffman, P.G.: On the stability of laminar flow of a dusty gas. *J. Fluid Mech.* **13**(1), 120–128 (1962)
2. Chakrabarti, K.M.: Note on boundary layer in a dusty gas. *AIAA J.* **12**(8), 1136–1137 (1974)
3. Vajravelu, K., Nayfeh, J.: Hydromagnetic flow of a dusty fluid over a stretching sheet. *Int. J. Non Linear Mech.* **27**(6), 937–945 (1992)
4. Chamkha, A.J.: The Stokes problem for a dusty fluid in the presence of magnetic field, heat generation and wall suction effects. *Int. J. Numer. Meth. Heat Fluid Flow* **10**(1), 116–133 (2000). <https://doi.org/10.1108/09615530010297958>
5. Attia, H.A.: Unsteady hydromagnetic channel flow of dusty fluid with temperature dependent viscosity and thermal conductivity. *Heat Mass Transf.* **42**(9), 779–787 (2006)
6. Damsheh, R.A.: On boundary layer flow of a dusty gas from a horizontal circular cylinder. *Braz. J. Chem. Eng.* **27**(4), 653–662 (2010)
7. Ezzat, M.A., El-Bary, A.A., Morsey, M.M.: Space approach to the hydro-magnetic flow of a dusty fluid through a porous medium. *Comput. Math. Appl.* **59**(8), 2868–2879 (2010)
8. Gireesha, B.J., Ramesh, G.K., Abel, M.S., Bagewadi, C.S.: Boundary layer flow and heat transfer of a dusty fluid flow over a stretching sheet with non-uniform heat source/sink. *Int. J. Multiph. Flow* **37**(8), 977–982 (2011)
9. Gireesha, B.J., Ramesh, G.K., Bagewadi, C.S.: Heat transfer in MHD flow of a dusty fluid over a stretching sheet with viscous dissipation. *J. Appl. Sci. Res.* **3**(4), 2392–2401 (2012)
10. Gireesha, B.J., Mahanthesh, B., Gorla, R.S.R.: Suspended particle effect on nanofluid boundary layer flow past a stretching surface. *J. Nanofluids* **3**(3), 267–277 (2014)
11. Manjunatha, P.T., Gireesha, B.J., Prasannakumara, B.C.: Effect of radiation on flow and heat transfer of MHD dusty fluid over a stretching cylinder embedded in presence of heat source. *Int. J. Appl. Comput. Math.* **3**(1), 293–310 (2017)
12. Turkyilmazoglu, M.: Magnetohydrodynamic two-phase dusty fluid flow and heat model over deforming isothermal surfaces. *Phys. Fluids* **29**(1), 013302 (2017)
13. Souayah, B., Kumar, K.G., Reddy, M.G., Rani, S., Hdhiri, N., Alfannakh, H., Rahimi-Gorji, M.: Slip flow and radiative heat transfer behavior of Titanium alloy and ferromagnetic nanoparticles along with suspension of dusty fluid. *J. Mol. Liq.* **290**, 11223 (2019)
14. Rashed, Z.Z.: Impacts of the properties heterogeneity on 3D magnetic dusty nanofluids flow within cubic porous enclosures contain isothermal cylinders. *Sci. Rep.* (2021). <https://doi.org/10.21203/rs.3.rs-967501/v1>

15. Ibrahim, M., Saeed, T., Bani, F., Sedeh, S.N., Chu, Y.-M., Toghraiee, D.: Two-phase analysis of heat transfer and entropy generation of water-based magnetite nanofluid flow in a circular microtube with twisted porous blocks under a uniform magnetic field. *Powder Technol.* **384**, 522–541 (2021). <https://doi.org/10.1016/j.powtec.2021.01.077>
16. Nazeer, M., Hussain, F., Khan, M.I., Shahzad, Q., Chu, Y.-M., Kadry, S.: MHD two-phase flow of Jeffrey fluid suspended with Hafnium and crystal particles: analytical treatment. *Numer. Methods Partial Differ. Eq.* **2021**, 1–18 (2021). <https://doi.org/10.1002/num.22766>
17. Walicki, E., Walicka, A.: Interia effect in the squeeze film of a couple-stress fluid in biological bearings. *Int. J. Appl. Mech. Eng.* **4**, 363–373 (1999)
18. Nagaraju, G., Ramana Murthy, J.V.: Mhd flow of Longitudinal and Torsional oscillations of a circular cylinder with suction in a couple stress fluid. *Int. J. Appl. Mech. Eng.* **13**, 1099–1114 (2013)
19. Nagarajua, G., Matta, A., Kaladhar, K.: Effects of chemical reaction and thermal radiation on heat generated stretching sheet in a couple stress fluid flow. *Front. Heat Mass Transf.* **7**, 1–5 (2016)
20. Asad, S., Alsaedi, A., Hayat, T.: Flow of couple stress fluid with variable thermal conductivity. *Appl. Math. Mech.* **37**(3), 315–324 (2016)
21. Jangili, S., Adesanya, S.O., Ogunseye, H.A., Lebelo, R.: Couple stress fluid flow with variable properties: a second law analysis. *Math. Methods Appl. Sci.* **42**(1), 85–98 (2019)
22. Aggarwal, A.K., Verma, A.: Effect of hall currents on thermal instability of dusty couple stress fluid. *Arch. Thermodyn.* **37**(3), 3–18 (2016)
23. Stanly, W., Vasantha Kumari, R.: Effect of rotation on dusty couple-stress fluid with hydromagnetic field heated below through porous medium. *World J. Eng.* **15**(1), 148–155 (2018)
24. Gajjela, N., Nandkeolyar, R.: Investigating the magnetohydrodynamic flow of a couple stress dusty fluid along a stretching sheet in the presence of viscous dissipation and suction. *Heat Transf.* **50**(3), 2709–2724 (2021). <https://doi.org/10.1002/htj.22001>
25. Munivenkatappa, U., Aswathanarayana, D.P., Sreevallabha Reddy, A., SureshBabu, R.: Effect of couple stress fluid in an irregular couette flow channel: an analytical approach. *Biointerface Res. Appl. Chem.* **12**(4), 4686 (2022)
26. Dogonchi, A.S., Waqas, M., Seyyedi, S.M., Hashemi-Tilehnoee, M., Ganji, D.D.: CVFEM analysis for $\text{Fe}_3\text{O}_4\text{—H}_2\text{O}$ nanofluid in an annulus subject to thermal radiation. *Int. J. Heat Mass Transf.* **132**, 473–483 (2019)
27. Seyyedi, S.M., Dogonchi, A.S., Nuraci, R., Ganji, D.D., Hashemi-Tilehnoee, M.: Numerical analysis of entropy generation of a nanofluid in a semi-annulus porous enclosure with different nanoparticle shapes in the presence of a magnetic field. *Eur. Phys. J. Plus.* **134**, 268 (2019)
28. Dogonchi, A.S., Hashemi-Tilehnoee, M., Waqas, M.: The Influence of different shapes of nanoparticle on $\text{Cu-H}_2\text{O}$ nanofluids in a partially heated irregular wavy enclosure. *Phys. A* (2019). <https://doi.org/10.1016/j.physa.2019.123034>
29. Mondal, S., Dogonchi, A.S., Tripathi, N., Waqas, M., Seyyedi, S.M., Hashemi-Tilehnoee, M., Ganji, D.D.: A theoretical nanofluid analysis exhibiting hydromagnetics characteristics employing CVFEM. *J. Braz. Soc. Mech. Sci. Eng.* **42**, 19 (2019). <https://doi.org/10.1007/s40430-019-2103-2>
30. Hashemi-Tilehnoee, M., Dogonchi, A.S., Seyyedi, S.M., Sharifpur, M.: Magneto-fluid dynamic and second law analysis in a hot porous cavity filled by nano fluid and nano-encapsulated phase change material suspension with different layout of cooling channels. *J. Energy Storage* **31**, 101720 (2020)
31. Sakiadis, B.C.: Boundary- layer behavior on continuous solid surfaces: I. Boundary layer equations for two- dimensional and axisymmetric flow. *AIChE J.* **7**(1), 26–28 (1961)
32. Crane, L.J.: Boundary layer flow due to a stretching cylinder. *Zeitschrift für angewandte Mathematik und Physik ZAMP.* **26**(5), 619–622 (1975)
33. Wang, C.Y.: Fluid flow due to a stretching cylinder. *Phys. Fluids* **31**(3), 466–468 (1988)
34. Mukhopadhyay, S.: MHD boundary layer slips flow along a stretching cylinder. *Ain Shams Eng. J.* **4**(2), 317–324 (2013)
35. Chauhan, D.S., Agrawal, R., Rastogi, P.: Magneto hydrodynamic slip flow and heat transfer in a Porous medium over a stretching cylinder: homotopy analysis method. *Numer. Heat Transf. Part A: Appl.* **62**(2), 136–157 (2012)
36. Nandkeolyar, R., Sibanda, P.: On convective dusty flow past a vertical stretching sheet with internal heat absorption. *J. Appl. Math.* **2013**, 806724 (2013). <https://doi.org/10.1155/2013/806724>
37. Punith Gowda, R.J., Naveen Kumar, R., Prasannakumara, B.C.: Two-phase darcy-forchheimer flow of dusty hybrid nanofluid with viscous dissipation over a cylinder. *Int. J. Appl. Comput. Math* **7**, 95 (2021). <https://doi.org/10.1007/s40819-021-01033-2>
38. Sinha, D., Jain, P., Siddheshwar, P.G.: Boundary layer flow and thermal analysis of a Cu-Nanofluid past a stretching cylinder. *Int. J. Appl. Comput. Math.* **3**, 2559–2572 (2017). <https://doi.org/10.1007/s40819-016-0255-7>

39. Gangadhar, K., Keziya, K., Rushi Kumar, B.: Effect of thermal radiation on heat transfer of ferrofluid over a stretching cylinder with convective heating. *Int. J. Eng. Technol.* **7**, 261–268 (2018)
40. Khan, M., Hashim, A.H.: Effects of thermal radiation and slip mechanism on mixed convection flow of williamson nanofluid over an inclined stretching cylinder. *Commun. Theor. Phys.* **71**, 1405–1415 (2019)
41. Ali, A., Kanwal, T., Awais, M., Shah, Z., Kumam, P., Thounthong, P.: Impact of thermal radiation and non-uniform heat flux on MHD hybrid nano fluid along a stretching cylinder. *Sci. Rep.* **11**, 20262 (2021). <https://doi.org/10.1038/s41598-021-99800-0>
42. Waqas, H., Imran, M., Muhammad, T., Sadiq, M., Ellahi, H.: On bio-convection thermal radiation in Darcy-Forchheimer flow of nanofluid with gyrotactic motile microorganism under Wu's slip over stretching cylinder/plate. *Int. J. Numer. Methods Heat Fluid Flow* (2020). <https://doi.org/10.1108/HFF-05-2020-0313>
43. Shahid, A., Bhatti, M.M., Ellahi, R., Mekheimer, Kh.S.: Numerical experiment to examine activation energy and bi-convection Carreau nanofluid flow on an upper paraboloid porous surface: application in solar energy. *Sustain. Energy Technol. Assess.* **52**, 102029 (2022)
44. Shehzad, N., Zeeshan, A., Shakeel, M., Ellahi, R., Sadiq Sait, M.: Effects of magneto hydrodynamics flow on multilayer coatings of newtonian and non-newtonian fluids through porous inclined rotating channel. *Coatings.* **12**, 430 (2022). <https://doi.org/10.3390/coatings12040430>
45. Zeeshan, A., Shehzad, N., Atif, M., Ellahi, R., Sait, S.M.: Electromagnetic flow of SWCNT/MWCNT suspensions in two immiscible water- and engine-oil-based newtonian fluids through porous media. *Symmetry.* **14**, 406 (2022). <https://doi.org/10.3390/sym14020406>
46. Makinde, O.D.: Effects of viscous dissipation and Newtonian heating on boundary layer flow of nano fluids over a flat plate. *Int. J. Numer. Meth. Heat Fluid Flow* **23**(8), 1291–1303 (2013). <https://doi.org/10.1108/HFF-12-2011-0258>
47. Farooq, M., Gull, N., Alsaedi, A., Hayat, T.: MHD flow of a Jeffrey fluid with Newtonian heating. *J. Mech.* **31**(3), 319–329 (2015)
48. Hayat, T., Hussain, Z., Alsaedi, A., Farooq, M.: Magneto hydrodynamic flow by a stretching cylinder with Newtonian heating and homogeneous-heterogeneous reactions. *Plosone.* **11**(6), e0156955 (2016)
49. Hayat, T., Khan, M.I., Waqas, M., Alsaedi, A.: Newtonian heating effect in nanofluid flow by a permeable cylinder. *Results Phys.* **7**, 256–262 (2017)
50. Nawaz, M., Zeeshan, A., Ellahi, R., Abbasbandy, S., Rashidi, S.: Joules and Newtonian heating effects on stagnation point flow over a stretching surface by means of genetic algorithm and Nelder-Mead method. *Int. J. Numer. Meth. Heat Fluid Flow* **25**(3), 665–684 (2015). <https://doi.org/10.1108/HFF-04-2014-0103>
51. Mishra, M., Panda, D., Swain, K.: Effects of joule heating and viscous dissipation on mhd flow and heat transfer of casson fluid over a stretching cylinder in a porous medium. *Int. J. Adv. Sci. Technol.* **29**(3), 9612–9623 (2020)
52. Zhao, T.-H., Khan, M.I., Chu, Y.-M.: Artificial neural networking (ANN) analysis for heat and entropy generation in flow of non-Newtonian fluid between two rotating disks. *Math. Meth Appl. Sci.* **2021**, 1–19 (2021). <https://doi.org/10.1002/mma.7310>
53. Qayyum, S., Khan, M.I., Masood, F., Chu, Y.-M., Kadry, S., Nazeer, M.: Interpretation of entropy generation in Williamson fluid flow with nonlinear thermal radiation and first-order velocity slip. *Math. Meth Appl. Sci.* **2020**, 1–10 (2019). <https://doi.org/10.1002/mma.6735>
54. Abbas, S.Z., Nayak, M.K., Mabood, F., Dogonchi, A.S., Chu, Y.-M., Khan, W.A.: Darcy Forchheimer electromagnetic stretched flow of carbon nanotubes over an inclined cylinder: Entropy optimization and quadratic chemical reaction. *Math. Meth Appl. Sci.* **2020**, 1–23 (2020). <https://doi.org/10.1002/mma.6956>
55. Song, Y.-Q., Waqas, H., Al-Khaled, K., Farooq, U., Khan, S.U., Ijaz Khan, M., Chu, Y.-M., Qayyum, S.: Bioconvection analysis for Sutter by nanofluid over an axially stretched cylinder with melting heat transfer and variable thermal features: a Marangoni and solutal model. *Alex. Eng. J.* **60**, 4663–4675 (2021). <https://doi.org/10.1016/j.aej.2021.03.056>

Publisher's Note Springer Nature remains neutral with regard to jurisdictional claims in published maps and institutional affiliations.

Springer Nature or its licensor holds exclusive rights to this article under a publishing agreement with the author(s) or other rightsholder(s); author self-archiving of the accepted manuscript version of this article is solely governed by the terms of such publishing agreement and applicable law.